Spin and phase coherence lengths in *n*-InSb quasi-one-dimensional wires

R. L. Kallaher* and J. J. Heremans†
Department of Physics, Virginia Tech, Blacksburg, Virginia 24061, USA

N. Goel, S. J. Chung, and M. B. Santos
Homer L. Dodge Department of Physics and Astronomy, University of Oklahoma, Norman, Oklahoma 73019, USA
(Received 16 August 2009; revised manuscript received 22 December 2009; published 29 January 2010)

We present measurements of the magnetoconductance of quasi-one-dimensional wires fabricated on a two-dimensional electron system in an InSb/InAlSb heterostructure. The width and temperature dependence of the spin and phase coherence lengths in the narrow wires are examined by analyzing the magnetoconductance in antilocalization theory, modified to account for ballistic transport. The experiments indicate that the confined geometry can enhance spin coherence lengths in systems not in the motional narrowing regime and in the presence of strong cubic Dresselhaus spin-orbit interaction. Experimentally, the spin coherence lengths are found to be inversely proportional to wire width and to display a weak temperature dependence. For all wire widths the phase coherence length, after correction for finite length effects, shows a temperature dependence indicative of phase decoherence via the one-dimensional Nyquist mechanism.

DOI: 10.1103/PhysRevB.81.035335 PACS number(s): 73.63.Nm, 72.25.Rb, 73.20.Fz, 73.23.Ad

I. INTRODUCTION

Recent theoretical studies[1–5] have predicted a suppression of spin-relaxation rates in narrow semiconducting channels fabricated from two-dimensional electron systems (2DESs). These predictions are supported by experiments performed on narrow wires fabricated from InGaAs (Ref. 6–8) and AlGaN/GaN 2DESs,[9] which have observed increasing spin coherence times τ_S as a function of reduced wire width w. For systems in the motional narrowing regime—for which a spin precesses only over a small angle between momentum scattering events—the spin coherence length L_S is expected to be inversely proportional to w.[3–5] Here we investigate the w dependence of L_S in quasi-one-dimensional (Q1D) wires, where w is shorter than the mean-free path l_e. The wires were fabricated on an InSb 2DES contained in an InSb/InAlSb heterostructure. The strong spin-orbit interactions (SOIs) and the high electron mobility in the InSb quantum well allow us to examine the dependence of L_S on w in a system that is not in the motional narrowing regime and where $w<l_e$.

We present measurements of magnetotransport at low magnetic fields in Q1D InSb wires. The dependence on temperature T and on w of L_S and of the phase coherence length L_ϕ are investigated by analyzing the wires' low-field magnetoconductance with low-dimensional antilocalization theory. Antilocalization theory describes deviations from the classically predicted conductance G_0 as a consequence of interference between itinerant electrons on time-reversed trajectories.[5,10–23] The magnitude of the antilocalization corrections depend on L_S, on L_ϕ, and on the applied magnetic field B. Thus quantitative information about both L_S and L_ϕ can be obtained from magnetotransport measurements.[5,10–23] Extensive experimental and theoretical research on antilocalization phenomena in thin films of metals[11–13] and semiconductors,[23–25] in 2DESs,[14–20,26–32] in hole systems,[22,33] and in narrow wires[7–9,34–36] demonstrate that these measurements form a valuable experimental tool for investigating spin and phase coherence in various material systems.

II. EXPERIMENT

Using lithographic techniques, Q1D wires of length $L=24\ \mu$m with nominal lithographic design widths, w_{litho}, between 0.475–0.875 μm were fabricated from an InSb/InAlSb n-type heterostructure grown by molecular-beam epitaxy on a GaAs (001) substrate. The 25 nm wide InSb quantum well, situated 163 nm below the surface of the heterostructure, is separated from Si δ-doped layers on either side by 40-nm-thick $In_{0.85}Al_{0.15}Sb$ barrier layers. An additional Si δ-doped layer is located 23 nm below the surface and balances surface states.[37] The wires are oriented along the $[1\bar{1}0]$ direction, as ascertained from the anisotropic profiles of a lactic/hydrofluoric/peroxide acid etch test. Data from four different wire sets (all fabricated on the same chip) are presented and discussed in this paper. Each set contains ten parallel wires of identical dimensions. The difference between sets of wires resides in the wire width. The data presented in this paper have been appropriately scaled and are presented in terms of conductance G per wire.

Magnetotransport across the wire sets was measured using standard low-frequency lock-in techniques for 0.4 K $<T<15$ K. In addition, four terminal resistivity and Hall-effect measurements were performed on an unpatterned region of the 2DES at each T. The unpatterned region shows a carrier density $n_{2D}\approx 5.2\times10^{15}$ m^{-2} and a mobility $\mu_{2D}\approx 9.7$ m^2/V s at 0.4 K. Antilocalization measurements performed on the unpatterned 2DES (Ref. 37) indicate that SOI in this material can be attributed to a combination of the Rashba[38,39] and cubic Dresselhaus terms.[39,40] The linear Dresselhaus term has little effect in this particular heterostructure, as it is largely canceled by a portion of the cubic Dresselhaus term.[37] The strength of the SOI in this 2DES is characterized by a Rashba parameter $|\alpha|\approx 0.03$ eV Å and a Dresselhaus parameter $\gamma\approx 490$ eV Å^3.[37] Using these values, we calculate the average SOI induced spin precession frequency in the 2DES as $\Omega\approx 2.5\times10^{12}$ s^{-1}. The spin precession length is calculated using the Fermi velocity $v_F\approx 8.85$

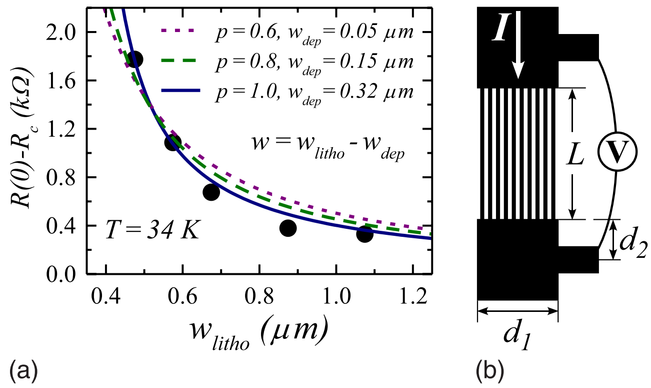

FIG. 1. (Color online) Wire set resistance $R(B=0)-R_c$ at $T=34$ K as a function of lithographic design width. $R(0)$ represents the measured resistance across the wire set and $R_c=114\ \Omega$ the series contact resistance estimated from $\rho_{2D}(34\ \text{K})$. A few comparative curves calculated from Eq. (1) are depicted along with the data. Right: schematic illustration of wire set geometry. From the ratio $d_2/d_1\approx 0.5$ we estimate $R_c\approx\rho_{2D}$.

$\times 10^5$ m/s, as $L_\Omega = v_F/\Omega \approx 0.35$ μm taking into account both the Rashba and Dresselhaus SOI. Hence, $L_\Omega \ll l_e = v_F\tau_p \approx 3.3$ μm, where $\tau_p \approx 3.7$ ps represents the momentum scattering time derived from μ_{2D} at $T=0.4$ K.

III. CHARACTERIZATION OF TRANSPORT PROPERTIES

In narrow wires, the carrier concentration n and mobility μ may differ from n_{2D} and μ_{2D} in the parent 2DES.[36,41,42] In the InSb wire sets, however, measurements of Shubnikov-De Haas oscillations at 0.4 K indicate no systematic change in n as a function of w. The measurements show that within $\sim$5% for all wires, $n=n_{2D}$, and hence for all wires we use $n=n_{2D}$ as determined at each T via Hall measurements on the unpatterned 2DES.

Two further effects enter in the determination of the wires' conductance. First, a series resistance due to the unpatterned entry and exit 2DES regions at both ends of the wires (Fig. 1) must be estimated and subtracted from the four-terminal wire resistance measurement. This effective series contact resistance R_c originates from the resistive voltage drop across the wide areas on either side of the wire sets. The area has a width $d_1=15$ μm. The distance d_2 between the end of the wires and the center of the voltage probes is $d_2\approx 7.5$ μm and hence $d_2/d_1\approx 0.5$. Taking into account twice a half-square sheet resistance leads to the estimate $R_c \approx \rho_{2D}$, where $\rho_{2D}=(1/n_{2D}e\mu_{2D})$ represents the resistivity of the parent 2DES. Second, the conducting width w can differ from the lithographic w_{litho} through edge depletion of carriers and processing effects encountered during the fabrication. By subtracting the depletion width w_{dep} from w_{litho}, w can be determined as $w=w_{litho}-w_{dep}$. In order to determine w, we examined the measured zero-field resistance $R(0)$ (corrected for R_c) across the different wire sets at $T\approx 34$ K where phase-coherent effects, such as antilocalization, are minimal. Figure 1 displays $R(0)$ as a function of w_{litho}. If n and μ are unaffected by the reduced dimensions, $R(0)$ should be inversely proportional to wire width according to the simple relation $R(0)-R_c=(L\rho_{2D}/w)$. However, diffusive boundary scattering from the wire's side walls can affect the diffusion constant D in narrow wires[41] and lead to a correction to $R(0)-R_c$. For purely specular boundary scattering, D is unchanged from the two-dimensional expression, $D=D_s=\frac{1}{2}v_F l_e$. For purely diffusive boundary scattering however,[41] $D_d=D_s\{1-\frac{4l_e}{\pi w}\int_0^1 x\sqrt{1-x^2}[1-\exp(-w/xl_e)]dx\}$. According to a model that accounts for both specular and diffusive boundary scattering, $R(0)-R_c$ as a function of w can be expressed as[43]

$$R(0)-R_c=\frac{L\rho_{2D}}{N_p w}\left[p+\frac{D_s}{D_d}(1-p)\right], \tag{1}$$

where p represents the probability for purely specular boundary scattering and $N_p=10$ the number of parallel wires. Equation (1) reduces to the limiting expressions[41,43] for either purely specular ($p=1$) or purely diffusive ($p=0$) boundary scattering. Since ρ_{2D} and l_e are determined by measurements on the unpatterned portion of the sample and L follows from the wire dimensions, only p and w form adjustable parameters in Eq. (1). Using a least-squares fit of Eq. (1) to the experimentally determined values of $R(0)$ at $T\approx 34$ K, we find the data are best explained by purely specular boundary scattering with an average depletion width $w_{dep}=0.32$ μm in the wires, Fig. 1. And, D equals D_s and can be assumed equal to its value measured in the unpatterned 2DES. Purely specular boundary scattering is consistent with a large w_{dep}, as the carriers are isolated from the roughness of the wire edges. It should be emphasized, however, that w_{dep} may not be entirely electrical in nature, as w_{dep} also includes effects from the fabrication process.

IV. CONDUCTANCE IN APPLIED *B*

Some examples of the low-field magnetoconductance $\Delta G \equiv G(B)-G(B=0)$ obtained at different T are depicted in Fig. 2. From the measurement geometry (Fig. 1) $G(B)$ for $T\leq 15$ K has been calculated from measured values of $R(B)$ assuming $R_c=125$ Ω, consistent with $\rho_{2D}(T\leq 15\ \text{K})$. In order to account for slight but inevitable Hall-effect contributions to the data, the component antisymmetric in B has been subtracted from the data by averaging $G(+B)$ and $G(-B)$ for each data set and hence ΔG is plotted in terms of the magnitude of the applied field, $|B|$. Antilocalization is observed in all the wire sets as evidenced by the negative magnetoconductance around $B=0$, crossing over to positive magnetoconductance at a higher $B=B_{cr}$. In 2DESs, the magnitude of the crossover field B_{cr} scales as L_S^{-2}.[11–13,15,17] In narrow wires, however, ΔG can be broadened since the one-dimensional magnetic length L_B is inversely related to w.[5,41] A detailed description of L_B in diffusive and ballistic wires can be found in Ref. 41. Briefly, phase coherence between time-reversed electrons is destroyed when the flux enclosed by the time-reversed trajectory $\Phi\sim h/e$. In narrow wires, the area of such trajectories can be characterized by wL_B as motion in the direction transverse to the wire axis is constrained by the wire boundaries. Thus, phase coherence is lost for trajectories where $\Phi=BwL_B=h/e$, leading to $L_B\sim 1/w$. In comparison to diffusive wires, the dependence of L_B on w in ballistic

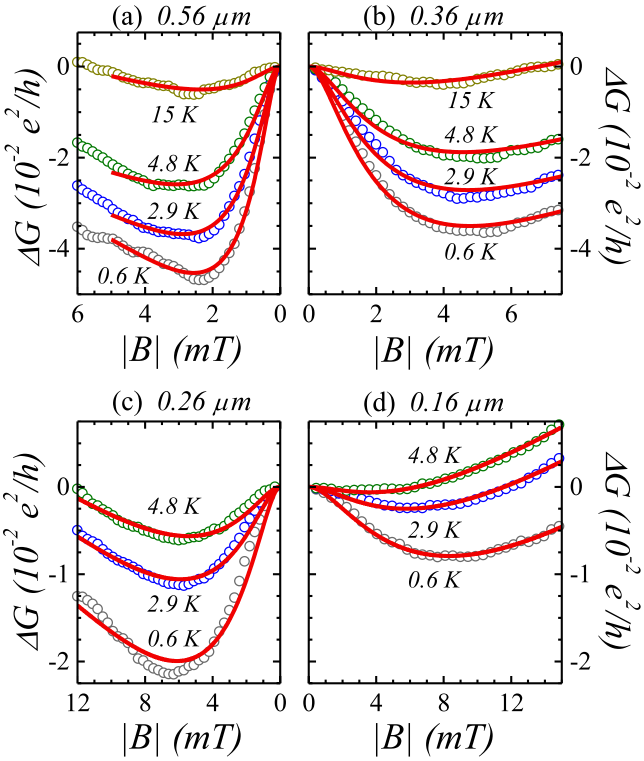

FIG. 2. (Color online) Change in conductance, ΔG, as a function of the magnitude of the applied magnetic field, $|B|$, at various T for four different wire widths w: (a) $w=0.56$ μm, (b) $w=0.36$ μm, (c) $w=0.26$ μm, and (d) $w=0.16$ μm. Solid lines are fits of the magnetoconductance traces to antilocalization theory.

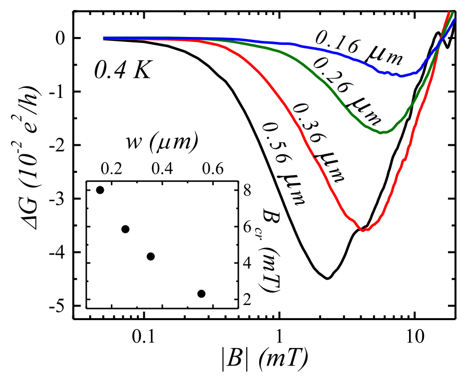

FIG. 3. (Color online) ΔG at 0.4 K, parametrized by the four wire widths. The inset plots the crossover field B_{cr}, at which negative magnetoconductance crosses over to positive magnetoconductance, as a function of wire width.

wires can be even stronger due to the *flux cancellation* effect which is a consequence of self-intersecting backscattered time-reversed trajectories.[36,41] Such trajectories can be visualized as being comprised of smaller distinct loops which the backscattered charge traverses in opposite directions.[41] In an applied field, the separate Aharonov-Bohm phases acquired by the charge as it encircles each of the smaller loops largely cancel since the sign of the phase depends on propagation direction. Thus, under flux cancellation a larger B is required to accumulate the same phase difference between such time-reversed trajectories and leads to further broadening of the $\Delta G(B)$ traces as a function of w. Figure 3 depicts the broadening of ΔG with narrowing w explicitly. The factor of 4 increase in B_{cr} as w decreases is a consequence of the w dependence of L_B in the narrow wires and is not indicative of a dramatic decrease in L_S.

Figure 3 also shows a decrease in the magnitude of the negative magnetoconductance for decreasing w. Negative magnetoconductance at low $|B|$ forms a characteristic feature of antilocalization under SOI and the magnitude of the antilocalization signal can be quantified as the observed $|\Delta G(B_{cr})|$. For $w=0.16$ μm, $|\Delta G(B_{cr})|$ is a factor ~ 6 smaller than for $w=0.56$ μm. A suppression of antilocalization in narrow wires has been previously observed in other systems.[7–9,35] In addition, the narrowest wires show the strongest T dependence of the negative magnetoconductance around $B=0$. Negative magnetoconductance is not observed above 5 K in the narrowest wires but is still evident at 15 K in the wider wires, according to Fig. 2. In 2DESs under SOI, $|\Delta G(B_{cr})|$ increases with the ratio L_ϕ/L_S. Thus the comparative magnitude and the T dependence of the negative magnetoconductance, between the wide and narrow wires, indicate a smaller ratio L_ϕ/L_S in the narrower wires.

Analysis

Under antilocalization, the total correction to G is composed of contributions from three triplet states and a singlet state.[5,15–21,23,44,45] The singlet contribution, which is sensitive to L_ϕ but not L_S, gives rise to negative magnetoconductance around zero field.[17] In contrast, the triplet contributions depend on both L_ϕ and L_S and are responsible for positive magnetoconductance. In materials with strong SOI, the singlet term dominates around $B=0$ and a negative magnetoconductance is observed. With increasing B the triplet contributions grow in relevance until they dominate and positive magnetoconductance is observed.[17] In Q1D systems, both the triplet and singlet contributions can be related to effective length scales[21,44,45] and the B dependence of G is then described by[5,21,36,41,44,45]

$$G(B) = G_0 - \frac{e^2}{hL}\left(\sum_{m=\pm 1,0} \tilde{L}_{1,m} - \tilde{L}_{0,0}\right), \tag{2}$$

where $\tilde{L}_{1m}$ represent the individual triplet length scales, $\tilde{L}_{00}$ is the singlet length scale, and L is the length of the wire. From Kettemann's formulation of antilocalization, the triplet and singlet length scales in wires fabricated from a 2DES are given by[5]

$$\tilde{L}_{s,m} = (L_\phi^{-2} + \nu_{s,m} L_S^{-2} + L_B^{-2})^{-1/2} \tag{3}$$

with $\nu_{1,\pm 1}=0.5$, $\nu_{1,0}=1$, and $\nu_{0,0}=0$. The B dependence of $G(B)$ is contained in the one-dimensional magnetic length $L_B = l_m\sqrt{1+3l_m^2/w^2}$, where $l_m=\sqrt{\hbar/eB}$ represents the magnetic length in two and three dimensions. This model is derived for $w < L_\Omega$.[5] However, experiments on InGaAs wires have indicated that the model can also model $G(B)$ in wires where $w \approx L_\Omega$.[8]

Kettemann's model was developed for diffusive wires where $l_e < w$. However, $l_e \gg w$ in the ballistic Q1D wires discussed here. Therefore, we implement the correction for ballistic wires first introduced by Beenakker[41] in weak localization theory. The triplet and singlet length scales in ballistic Q1D wires then become[41]

$$\tilde{L}_{s,m} = (L_\phi^{-2} + \nu_{s,m}L_S^{-2} + L_B^{-2})^{-1/2} - (L_\phi^{-2} + \nu_{s,m}L_S^{-2} + L_B^{-2} + 2l_e^{-2})^{-1/2}, \tag{4}$$

where, again, we take $\nu_{1,\pm 1}=0.5$, $\nu_{1,0}=1$, and $\nu_{0,0}=0$.[5] In ballistic rather than diffusive Q1D wires, L_B is described by[41]

$$L_B = l_m \sqrt{\frac{C_1 l_m^2 l_e}{w^3} + \frac{C_2 l_e^2}{w^2}}. \tag{5}$$

The values of the numerical constants C_1 and C_2 depend on whether the boundary scattering is specular or diffusive, with $C_1=4.75(2\pi)$ and $C_2=2.4(1.5)$ for predominately specular (diffusive) boundary scattering.[41] Equation (5) accounts for the flux cancellation effect in ballistic wires.[41]

In order to extract L_S and L_ϕ, the magnetoconductance curves were fit to Eq. (2) using Eq. (4) to describe $\tilde{L}_{s,m}$. L_B was evaluated by Eq. (5), using specular boundary scattering values for C_1 and C_2. The resulting fits are depicted along with the experimental data in Fig. 2. The extracted values for L_S and L_ϕ are presented below, and their dependence on w and T discussed in detail.

We note that fitting the magnetoconductance data to Kettemann's model[5] without implementing the two ballistic modifications leads to substantially different L_S and L_ϕ. By separately examining the effect of each of the two modifications on the results, we find that the ballistic L_B is primarily responsible for the difference. Applying a ballistic L_B in wires where $l_e \gg w$ is well established in the literature[34,36,41,43,46–48] and is thus appropriate for the study of antilocalization in the Q1D InSb wires presented here, up to widths $w=0.56$ μm.

V. RESULTS

A. Spin coherence length

Values for L_S extracted from the ballistic model are found to range between ~3–5 μm, with L_S increasing as w narrows. The dependence of L_S on w at 0.4 and 1.3 K is depicted in Fig. 4. Since L_Ω has a constant value of 0.35 μm over the range of the experiments, Fig. 4 shows that L_S follows $L_S \propto w^{-1}$. The dependence is valid up to $T\approx 5$ K (above 5 K antilocalization was not observed for $w \leq 0.26$ μm). Although an increase in L_S with decreasing w has been previously observed in narrow wires where Rashba SOI limits L_S,[6–8] here we find the same behavior in the presence of strong cubic Dresselhaus SOI, in ballistic InSb Q1D wires, and where $L_\Omega \ll l_e$.

We can estimate the enhancement of L_S over its value L_S^{2D} in an unpatterned 2DES. Given the strong SOI in the system, the L_S observed in the wires are seemingly quite long. However, in systems with a long l_e, and where $L_\Omega < l_e$, one would not expect spin decoherence to occur on a time scale much shorter than τ_p.[18] For 2DESs where $L_\Omega < l_e$, it is common to estimate $\tau_S^{2D} \approx \tau_p$, as a rapid spin precession frequency is

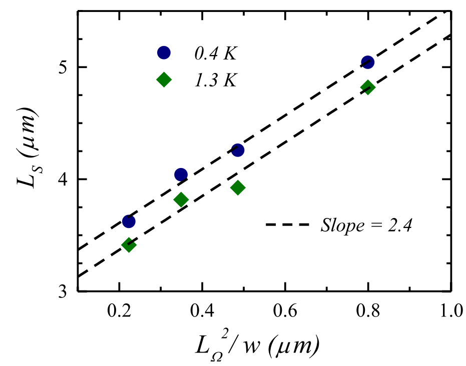

FIG. 4. (Color online) Dependence of the spin coherence length L_S on wire width w and on spin precession length $L_\Omega \approx 0.35$ μm, at T=0.4 and 1.3 K.

assumed to cause decoherence promptly after the first random scattering event occurs.[4,49,50] Unlike in the motional narrowing regime, $\tau_S^{2D} \approx \tau_p$ suggests that decreased momentum scattering leads to a longer L_S^{2D}. At 0.4 K, the above estimate predicts $L_S^{2D} \equiv \sqrt{D\tau_S^{2D}} \approx \sqrt{D\tau_p} \approx 2.5$ μm. Thus, for the narrowest wires ($w \approx 0.16$ μm) we find a factor of ≈ 2 enhancement in L_S as compared to the estimated L_S^{2D}.

From the data in Fig. 4, it follows that $L_S \propto 2.4(L_\Omega^2/w)$. The proportionality factor 2.4 holds, within experimental error, up to $T \approx 5$ K. As has been observed previously,[8] L_S is enhanced even in wires where $w > L_\Omega$. We are not aware of theoretical predictions for enhanced L_S in ballistic wires which consider both Rashba and cubic Dresselhaus SOI. However, accounting for the two different SOI contributions, Kettemann[5] predicts that the dimensional confinement in narrow diffusive wires leads to a dependence of L_S on w as

$$\frac{1}{L_S^2}(w) = \frac{1}{L_\gamma^2} + \frac{w^2}{12 L_\Omega^2 L_R^2} \tag{6}$$

with $L_R = v_F/\Omega_R$ and $L_\gamma = v_F/\Omega_\gamma$, where $\Omega_R = 2|\alpha|k_p/\hbar$ and $\Omega_\gamma = \gamma k_p^3/2\hbar$ with $k_p = \sqrt{2\pi n}$ the wave vector in the 2DES plane. Ω_R and Ω_γ represent the respective spin precession frequencies associated with the Rashba and cubic Dresselhaus SOI in the parent 2DES [the linear Dresselhaus term has little effect in this particular InSb 2DES (Ref. 37) and has been neglected]. For pure Rashba SOI, when $L_\gamma^{-1}=0$ and $L_R = L_\Omega$, Eq. (6) predicts that dimensional confinement enhances L_S with the dependence $L_S \propto \sqrt{12}(L_\Omega^2/w)$. However, the strong cubic Dresselhaus SOI in InSb leads to a small L_γ and, thus, is expected to *largely* inhibit the enhancement of L_S due to dimensional confinement.[5,6] The observed significant increase in L_S as w decreases from 0.56 to 0.26 μm indicates the L_γ^{-2} term of Eq. (6) is greatly suppressed for the ballistic InSb wires. Furthermore, the experimentally observed dependence $L_S \propto 2.4(L_\Omega^2/w)$, is in agreement, within $\approx\sqrt{2}$, of the prediction for the enhancement of L_S due to dimensional confinement. Since L_Ω has been calculated accounting for both Rashba and cubic Dresselhaus SOI, we conclude that in the ballistic InSb wires dimensional confinement not only affects spin relaxation due to Rashba SOI but that it similarly suppresses spin relaxation arising from cubic

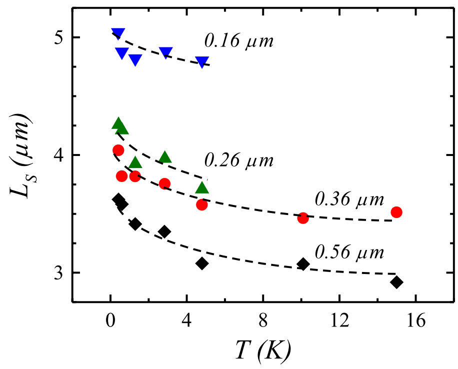

FIG. 5. (Color online) Spin coherence length L_S as a function of T for four values of the wire width. Dashed lines form guides to the eye.

Dresselhaus SOI. However, the effect of dimensional confinement on spin relaxation due to cubic Dresselhaus SOI is an unresolved issue.[5,6,8] Antilocalization studies on narrow InGaAs wires[8] have also suggested a large suppression of the L_γ^{-2} term in Eq. (6). In contrast, spin relaxation probed by optical time-resolved Faraday rotation spectroscopy[6] have indicated that cubic Dresselhaus SOI may, in fact, limit the enhancement of L_S in InGaAs wires.

The dependence of L_S on T for the four separate wire widths is depicted in Fig. 5. A weak T dependence of L_S is observed for all w, with L_S gradually decreasing as T increases. Since experimentally all wires follow a similar T dependence and since the enhancement L_S/L_S^{2D} is independent of T in the experimental range, the decrease in L_S with increasing T is presumed to originate in the same mechanisms that limit L_S^{2D}. As mentioned above, because $L_\Omega < l_e$ in the parent InSb/InAlSb heterostructure, a reduction in L_S^{2D} implies an increase in scattering. Both phonon and electron-electron scattering are expected to increase with T and offer mechanisms for decreasing L_S^{2D}. It has been noted that scattering mechanisms can show a much larger impact on spin relaxation as compared to momentum relaxation.[51] Even though the increase in phonon and electron-electron scattering with T do not result in an observable effect on l_e in the experimental range of T, yet the antilocalization data do suggest an effect on L_S.

B. Phase coherence length

Figures 6 and 7 contain the dependence of L_ϕ on T observed in the InSb wires. For all w, L_ϕ follows a similar T dependence, with L_ϕ decreasing with increasing T. The similarity of the T dependence of L_ϕ in the different wires is portrayed in a logarithmic plot of L_ϕ, normalized to its value at 0.4 K, versus T (inset of Fig. 6). After normalization to L_ϕ(0.4 K) the data from all wires collapse onto a single curve, within experimental errors.

The inset of Fig. 6 and the logarithmic plots of L_ϕ versus T displayed in Fig. 7 reveal that L_ϕ approaches a constant value ($L_\phi \approx 8$ μm) as $T \to 0$. Phase coherence phenomena have been investigated in 2DESs (Ref. 26) and hole systems,[52] wires,[34,43,46,47,53] and quantum dots.[54,55] Often it is

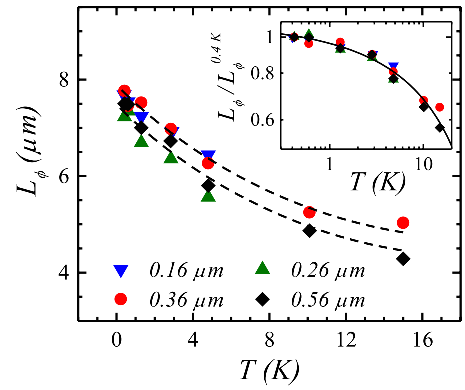

FIG. 6. (Color online) T dependence of the phase coherence length L_ϕ in wires with four different widths. Dashed lines for widths of 0.36 and 0.56 μm form guides to the eye. Inset: logarithmic plot of the T dependence of L_ϕ, normalized by its value at 0.4 K, for all wires.

reported that the phase coherence time τ_ϕ, where $L_\phi \equiv \sqrt{D\tau_\phi}$, approaches a constant value as $T \to 0$. Various mechanisms have been invoked to explain the saturation of L_ϕ and τ_ϕ at low T. Such mechanisms include magnetic scattering from trace magnetic impurities[46] and zero-point fluctuations of the electromagnetic environment.[56] The overall experimentally determined dependence of L_ϕ on T can be captured by[46]

$$\left(\frac{1}{L_\phi}\right)^2 = \left(\frac{1}{L_\phi^0}\right)^2 + \left(\frac{1}{L_\phi^T(T)}\right)^2, \tag{7}$$

where L_ϕ^0 is a constant. The entire T dependence of L_ϕ is then contained in $L_\phi^T(T)$, often observed to follow a power law, $L_\phi^T(T) \propto T^{-\nu}$. The exponent ν characteristically depends on the dominant phase decoherence mechanism.[46]

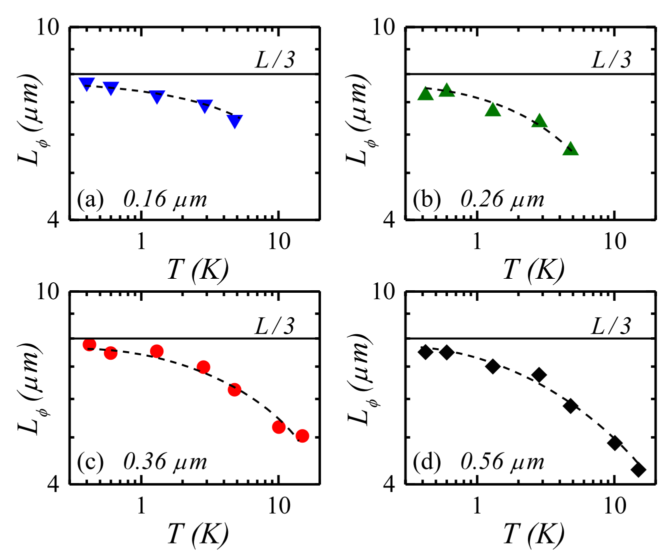

FIG. 7. (Color online) Logarithmic plot of L_ϕ vs T for the InSb wires of width (a) 0.16 μm, (b) 0.26 μm, (c) 0.36 μm, and (d) 0.56 μm. Dashed lines form guides to the eye. In all wires L_ϕ appears to be limited by $L/3 = 8$ μm (solid line) as $T \to 0$.

In the experimental range of T for the InSb wires, the term in L_ϕ^0 in Eq. (7) has a determining effect on L_ϕ. Furthermore, Fig. 7 demonstrates that the saturation value L_ϕ^0 is largely independent of w, leading to a lack of a clear dependence of L_ϕ on w in the experimental data. Below we will show that the observed saturation, resulting in $L_\phi \rightarrow L_\phi^0 \approx 8$ μm as $T \rightarrow 0$, originates in the finite size of the InSb wires. Previous investigations on GaAs wires[57] have similarly reported an L_ϕ limited by wire geometry.

We have so far described $\Delta G(B)$ by a model developed for Q1D wires of infinite length ($L \gg L_\phi$). Investigations of localization phenomena have revealed that $\Delta G(B)$ in finite length wires can be influenced by the specific geometry of the wires and the corresponding current and voltage measurement probes.[57–60] These studies have suggested that the L_ϕ extracted by fitting $\Delta G(B)$ measured in finite length wires to an infinite wire model, represents an effective phase coherence length, determined by both L and by an inherent phase coherence length λ_ϕ. Here λ_ϕ is determined by phase decoherence mechanisms intrinsic to the material and is independent of wire length. In the limit $w \ll \lambda_\phi$, the relationship between the effective measured L_ϕ and the intrinsic λ_ϕ in finite wires can be described by[57–60]

$$\frac{L_\phi}{L} = \frac{\lambda_\phi}{L}\coth\left(\frac{L}{\lambda_\phi}\right) - \frac{\lambda_\phi^2}{L^2}. \tag{8}$$

For Q1D channels, Nyquist dephasing often dominates at low T.[46] Nyquist dephasing results from the interaction of a given conduction electron with the fluctuating electromagnetic field generated by surrounding electrons and in one dimension theoretically gives rise to[46,61]

$$\frac{1}{\lambda_\phi} = \left(\frac{k_B T}{\hbar^2 D^2 g(0) w}\right)^{1/3}, \tag{9}$$

where $g(0)$ represents the density of states at the Fermi level and k_B is the Boltzmann constant. As upon lowering T, $\lambda_\phi / L > 1$, the right side of Eq. (8) converges to a constant value of 1/3. Thus, for the present InSb wires, it can be expected that as $T \rightarrow 0$ the extracted $L_\phi \rightarrow L_\phi^0 = L/3 \approx 8$ μm. Indeed, Fig. 7 suggests that for all wires L_ϕ is limited by $L/3$ as $T \rightarrow 0$. Equation (8) can be approximated by $L_\phi^{-2} \approx \lambda_\phi^{-2} + \pi^2 L^{-2}$ (Ref. 57) and, thus, can be related to Eq. (7) by equating $\lambda_\phi = L_\phi^T$.

Equation (8) characterizes the finite-size correction for the singlet term and L_ϕ. Similar corrections apply to the triplet terms which depend on L_S.[58,59] To determine how the finite size of the wires affects L_ϕ (λ_ϕ) and L_S, the measured $\Delta G(B)$ curves were fit to Eq. (2) using correction factors of the form given in Eq. (8) for both $(L_\phi^{-2} + L_B^{-2})^{-1/2}$ and $(L_\phi^{-2} + \nu_{1,m} L_S^{-2} + L_B^{-2})^{-1/2}$. Values for λ_ϕ obtained from the fits after correction for finite L are displayed as a function of T in Fig. 8. Figure 8 shows that λ_ϕ in all wires follows a $T^{-1/3}$ dependence. The fact that λ_ϕ in all four sets of wires agree with a $T^{-1/3}$ law suggests that the Nyquist mechanism is indeed responsible for phase decoherence in the InSb wires. In contrast to L_ϕ, these fits reveal that the values for L_S are relatively unaffected ($<5\%$) by the finite length of the InSb wires.

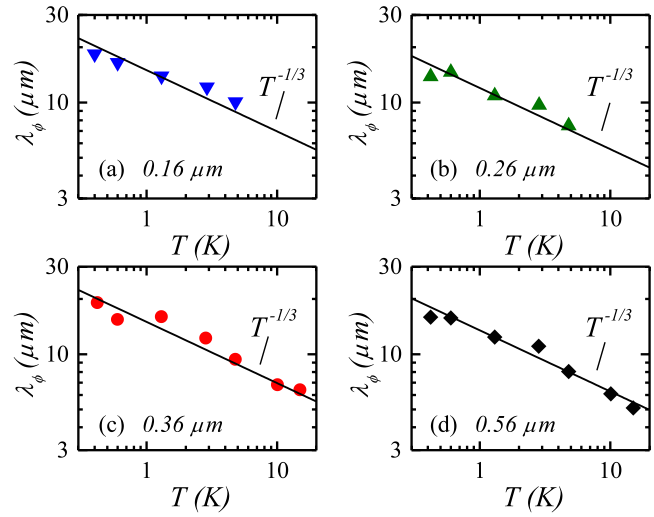

FIG. 8. (Color online) Logarithmic plot of λ_ϕ vs T for the InSb wires of width (a) 0.16 μm, (b) 0.26 μm, (c) 0.36 μm, and (d) 0.56 μm. In all wires λ_ϕ can be described by a $T^{-1/3}$ law.

VI. CONCLUSIONS

The coherence lengths L_S and L_ϕ in Q1D wires patterned on an InSb 2DES are investigated through analysis of antilocalization phenomena, using a model modified for ballistic transport. Concerning wire widths, a dependence $L_S \propto w^{-1}$ is observed. $L_S \propto w^{-1}$ is predicted for diffusive wires in the motional narrowing regime and is here observed for ballistic wires ($w < l_e$) in which $L_\Omega < l_e$. For $w = 0.16$ μm, a factor ≈ 2 enhancement of L_S over unpatterned 2DES is measured. As expected for wires of finite length, L_ϕ in all wires saturates to $L_\phi \rightarrow L/3 = 8$ μm as $T \rightarrow 0$, with little or no observed dependence on w. The Nyquist mechanism dominates intrinsic phase decoherence.

ACKNOWLEDGMENTS

This work is supported by the DOE through Grant No. DE-FG02-08ER46532 and by the NSF through Grants No. DMR-0618235 and No. DMR-0520550.

*kallaher@vt.edu
†heremans@vt.edu

[1] A. Bournel, P. Dollfus, P. Bruno, and P. Hesto, Eur. Phys. J.: Appl. Phys. **4**, 1 (1998).
[2] T. P. Pareek and P. Bruno, Phys. Rev. B **65**, 241305(R) (2002).
[3] A. G. Mal'shukov and K. A. Chao, Phys. Rev. B **61**, R2413 (2000).
[4] A. A. Kiselev and K. W. Kim, Phys. Rev. B **61**, 13115 (2000).

[5] S. Kettemann, Phys. Rev. Lett. **98**, 176808 (2007).
[6] A. W. Holleitner, V. Sih, R. C. Myers, A. C. Gossard, and D. D. Awschalom, Phys. Rev. Lett. **97**, 036805 (2006).
[7] Th. Schäpers, V. A. Guzenko, M. G. Pala, U. Zülicke, M. Governale, J. Knobbe, and H. Hardtdegen, Phys. Rev. B **74**, 081301(R) (2006).
[8] Y. Kunihashi, M. Kohda, and J. Nitta, Phys. Rev. Lett. **102**, 226601 (2009).
[9] P. Lehnen, Th. Schäpers, N. Kaluza, N. Thillosen, and H. Hardtdegen, Phys. Rev. B **76**, 205307 (2007).
[10] G. Bergmann, Phys. Rev. B **28**, 2914 (1983).
[11] G. Bergmann, Phys. Rep. **107**, 1 (1984).
[12] S. Hikami, A. I. Larkin, and Y. Nagaoka, Prog. Theor. Phys. **63**, 707 (1980).
[13] S. Kobayashi and F. Komori, Prog. Theor. Phys. Suppl. **84**, 224 (1985).
[14] K. S. Romanov and N. S. Averkiev, Zh. Eksp. Teor. Fiz. **128**, 811 (2005) [JETP **101**, 699 (2005)].
[15] S. V. Iordanskii, Yu. B. Lyanda-Geller, and G. E. Pikus, Pis'ma Zh. Eksp. Teor. Fiz. **60**, 199 (1994) [JETP Lett. **60**, 206 (1994)].
[16] A. Zduniak, M. I. Dyakonov, and W. Knap, Phys. Rev. B **56**, 1996 (1997).
[17] W. Knap, C. Skierbiszewski, A. Zduniak, E. Litwin-Staszewska, D. Bertho, F. Kobbi, J. L. Robert, G. E. Pikus, F. G. Pikus, S. V. Iordanskii, V. Mosser, K. Zekentes, and Yu. B. Lyanda-Geller, Phys. Rev. B **53**, 3912 (1996).
[18] J. B. Miller, D. M. Zumbühl, C. M. Marcus, Y. B. Lyanda-Geller, D. Goldhaber-Gordon, K. Campman, and A. C. Gossard, Phys. Rev. Lett. **90**, 076807 (2003).
[19] F. G. Pikus and G. E. Pikus, Phys. Rev. B **51**, 16928 (1995).
[20] L. E. Golub, Phys. Rev. B **71**, 235310 (2005).
[21] P. Santhanam, S. Wind, and D. E. Prober, Phys. Rev. B **35**, 3188 (1987).
[22] N. S. Averkiev, L. E. Golub, and G. E. Pikus, Zh. Eksp. Teor. Fiz. **113**, 1429 (1998) [JETP **86**, 780 (1998)].
[23] B. L. Al'tshuler, A. G. Aronov, A. I. Larkin, and D. E. Khmel'nitkskii, Zh. Eksp. Teor. Fiz. **81**, 768 (1981) [Sov. Phys. JETP **54**, 411 (1981)].
[24] L. P. Rokhinson, Y. Lyanda-Geller, Z. Ge, S. Shen, X. Liu, M. Dobrowolska, and J. K. Furdyna, Phys. Rev. B **76**, 161201(R) (2007).
[25] R. L. Kallaher and J. J. Heremans, Phys. Rev. B **79**, 075322 (2009).
[26] S. A. Studenikin, P. T. Coleridge, N. Ahmed, P. J. Poole, and A. Sachrajda, Phys. Rev. B **68**, 035317 (2003).
[27] T. Koga, J. Nitta, T. Akazaki, and H. Takayanagi, Phys. Rev. Lett. **89**, 046801 (2002).
[28] D. D. Bykanov, A. M. Kreshchuk, S. V. Novikov, T. A. Polyanskaya, and I. G. Savel'ev, Semiconductors **32**, 985 (1998).
[29] A. M. Kreshchuk, S. V. Novikov, T. A. Polyanskaya, and I. G. Savel'ev, Semiconductors **31**, 391 (1997).
[30] G. M. Minkov, A. V. Germanenko, O. E. Rut, A. A. Sherstobitov, L. E. Golub, B. N. Zvonkov, and M. Willander, Phys. Rev. B **70**, 155323 (2004).
[31] T. Hassenkam, S. Pedersen, K. Baklanov, A. Kristensen, C. B. Sorensen, P. E. Lindelof, F. G. Pikus, and G. E. Pikus, Phys. Rev. B **55**, 9298 (1997).
[32] V. A. Guzenko, M. Akabori, Th. Schäpers, S. Cabañas, T. Sato, T. Suzuki, and S. Yamada, Phys. Status Solidi C **3**, 4227 (2006).
[33] S. Pedersen, C. B. Sørensen, A. Kristensen, P. E. Lindelof, L. E. Golub, and N. S. Averkiev, Phys. Rev. B **60**, 4880 (1999).
[34] A. E. Hansen, M. T. Björk, C. Fasth, C. Thelander, and L. Samuelson, Phys. Rev. B **71**, 205328 (2005).
[35] A. Wirthmann, Y. S. Gui, C. Zehnder, D. Heitmann, C.-M. Hu, and S. Kettemann, Physica E (Amsterdam) **34**, 493 (2006).
[36] Ç. Kurdak, A. M. Chang, A. Chin, and T. Y. Chang, Phys. Rev. B **46**, 6846 (1992).
[37] R. L. Kallaher, J. J. Heremans, N. Goel, S. J. Chung, and M. B. Santos, Phys. Rev. B (to be published).
[38] Y. A. Bychkov and E. I. Rashba, J. Phys. C **17**, 6039 (1984).
[39] R. Winkler, in *Spin-Orbit Coupling Effects in Two-Dimensional Electron and Hole Systems* (Springer, Berlin, 2003).
[40] G. Dresselhaus, Phys. Rev. **100**, 580 (1955).
[41] C. W. J. Beenakker and H. van Houten, Phys. Rev. B **38**, 3232 (1988).
[42] K.-F. Berggren, G. Roos, and H. van Houten, Phys. Rev. B **37**, 10118 (1988).
[43] J. A. Katine, M. J. Berry, R. M. Westervelt, and A. C. Gossard, Phys. Rev. B **57**, 1698 (1998).
[44] P. Santhanam, S. Wind, and D. E. Prober, Phys. Rev. Lett. **53**, 1179 (1984).
[45] J. C. Licini, G. J. Dolan, and D. J. Bishop, Phys. Rev. Lett. **54**, 1585 (1985).
[46] J. J. Lin and J. P. Bird, J. Phys.: Condens. Matter **14**, R501 (2002).
[47] D. Liang, M. R. Sakr, and X. P. A. Gao, Nano Lett. **9**, 1709 (2009).
[48] M. Ferrier, L. Angers, A. C. H. Rowe, S. Guéron, H. Bouchiat, C. Texier, G. Montambaux, and D. Mailly, Phys. Rev. Lett. **93**, 246804 (2004).
[49] I. Žutić, J. Fabian, and S. Das Sarma, Rev. Mod. Phys. **76**, 323 (2004).
[50] V. N. Gridnev, JETP Lett. **74**, 380 (2001).
[51] M. A. Brand, A. Malinowski, O. Z. Karimov, P. A. Marsden, R. T. Harley, A. J. Shields, D. Sanvitto, D. A. Ritchie, and M. Y. Simmons, Phys. Rev. Lett. **89**, 236601 (2002).
[52] S. McPhail, C. E. Yasin, A. R. Hamilton, M. Y. Simmons, E. H. Linfield, M. Pepper, and D. A. Ritchie, Phys. Rev. B **70**, 245311 (2004).
[53] F. J. Ruess, B. Weber, K. E. J. Goh, O. Klochan, A. R. Hamilton, and M. Y. Simmons, Phys. Rev. B **76**, 085403 (2007).
[54] B. Hackens, S. Faniel, C. Gustin, X. Wallart, S. Bollaert, A. Cappy, and V. Bayot, Phys. Rev. Lett. **94**, 146802 (2005).
[55] J. P. Bird, A. P. Micolich, D. K. Ferry, R. Akis, Y. Ochiai, Y. Aoyagi, and T. Sugano, Solid-State Electron. **42**, 1281 (1998).
[56] P. Mohanty and R. A. Webb, Phys. Rev. B **55**, R13452 (1997).
[57] K. K. Choi, D. C. Tsui, and K. Alavi, Phys. Rev. B **36**, 7751 (1987).
[58] V. Chandrasekhar, D. E. Prober, and P. Santhanam, Phys. Rev. Lett. **61**, 2253 (1988).
[59] V. Chandrasekhar, P. Santhanam, and D. E. Prober, Phys. Rev. B **44**, 11203 (1991).
[60] B. L. Al'tshuler, A. G. Aronov, and A. Yu. Zyuzin, Zh. Eksp. Teor. Fiz. **86**, 709 (1984) [Sov. Phys. JETP **59**, 415 (1984)].
[61] B. L. Altshuler, A. G. Aronov, and D. E. Khmelnitsky, J. Phys. C **15**, 7367 (1982).